Proceedings of the ASME 2012 Summer Heat Transfer Conference
HT2012
July 8-12, 2012, Rio Grande, Puerto Rico

HT2012-58125

Experimental Investigation of Single-Phase Heat Transfer in a Horizontal Internally Micro-Fin Tube with Three Different Inlet Configurations

Hou Kuan Tam
Department of Electromechanical Engineering, Faculty of Science and Technology, University of Macau, Av. Padre Tomás Pereira, Taipa, Macau, China.

Lap Mou Tam
Department of Electromechanical Engineering, Faculty of Science and Technology, University of Macau, Av. Padre Tomás Pereira, Taipa, Macau, China.
Institute for the Development and Quality, Macau.

Afshin J. Ghajar
School of Mechanical and Aerospace Engineering, Oklahoma State University, Stillwater, Oklahoma, USA.

Cheong Sun
Department of Electromechanical Engineering, Faculty of Science and Technology, University of Macau, Av. Padre Tomás Pereira, Taipa, Macau, China.

Weng Kuong Lai
Department of Electromechanical Engineering, Faculty of Science and Technology, University of Macau, Av. Padre Tomás Pereira, Taipa, Macau, China.

ABSTRACT

To increase heat transfer, internally micro-fin tubes are widely used in commercial HVAC applications. It is commonly understood that the micro-fin enhances heat transfer in the turbulent region. There are only a few works that fundamentally studied the continuous change in the characteristic behavior of heat transfer from laminar to transition and eventually the turbulent regions. Furthermore, it is difficult to find the information about the effect of inlet configuration on the micro-fin tube heat transfer in the open literature. Therefore, more in-depth study for the micro-fin tube heat transfer characteristics is necessary.

In this study, heat transfer was measured in a single test section fitted with a micro-fin tube and compared with the data of a plain tube. Both of the tubes with the same internal diameter of 14.9 mm were tested under the uniform wall heat flux boundary condition. Three inlet configurations, re-entrant, square-edged, and bell-mouth, were used in this study. The entire experiment covered the Reynolds number range between 1100 and 23,000.

From the heat transfer results, the transition from laminar to turbulent region for the plain and micro-fin tubes was clearly established. For both of the plain and micro-fin tubes in the laminar region, buoyancy effects and heat transfer magnitudes were comparable. It was also observed that for the micro-fin tube heat transfer enhancement initiated in the transition region and lasted through the turbulent region.

For both of the plain and micro-fin tubes, the transition from laminar to turbulent region was found to be inlet dependent. For bell-mouth inlet, it was obvious that the micro-fin tube had an earlier transition than the plain tube. Furthermore, for both of the plain and micro-fin tubes with bell-mouth inlet, an unusual behavior of the local heat transfer coefficient was observed in the transition and turbulent regions.

INTRODUCTION

Single-phase liquid flow in internally enhanced tubes is becoming more important in commercial HVAC applications, where enhanced tube bundles are used in flooded evaporators and shell-side condensers to increase heat transfer. This enables water chillers to reach high efficiency, which helps mitigate global warming concerns of HVAC systems. One kind of internally enhanced tube is the micro-fin tube. Jensen and Vlakancic [1] defined the micro-fin tube to have a height less

than $0.03D_i$ (i.e. $2e/D_i<0.06$), where D_i is the inside tube diameter and e is the fin height. Basically, such kind of tube is widely used in high flow rate applications because the heat transfer enhancement in high flow rates (turbulent region) is more pronounced than that in the low flow rates (laminar region). Khanpara et al. [2] reported that the turbulent heat transfer in micro-fin tubes had an increase of 30 to 100% with Reynolds numbers between 5000 and 11,000. Brognaux et al. [3] indicated that there was a 65 to 95% increase in heat transfer for the micro-fin tube over the smooth tube. For the laminar flow, several researchers [3-6] concluded that the heat transfer was not greatly affected by micro-fins. Trupp and Haine [7] indicated that the secondary flow inside the tube with longitudinal fins was insignificant in the laminar flow and the thermal entry length was shown not to be relevant to the fin geometry.

For the micro-fin tubes, the tube side roughening increases the heat transfer surface area resulting in high efficiency heat exchangers. When compared to a plain tube with a constant pumping power, the tube side roughening also causes lower flow rates in the heat exchanger tubes, resulting in the flow to be at Reynolds numbers that are between laminar and turbulent, that is in the transition region. Owing to the high efficiency requirements, it is likely that more HVAC units will operate in the transition region where the understanding of the heat transfer is limited.

According to the plain tube studies done by Ghajar and his co-workers [8-10], the entrance flow, buoyancy, and the shape of inlet configuration influence the heat transfer in transition region flow. However, in the past studies of micro-fin tubes, some of the above-mentioned points were always ignored. Therefore, Tam et al. [11] conducted the heat transfer and friction factor experiments for micro-fin tubes to address those points. In their study, only the re-entrant and square-edged inlets were used and hence there was no information about effect of the bell-mouth inlet on the micro-fin tube heat transfer. In fact, for the plain tube with bell-mouth inlet, the unusual behavior of the local heat transfer coefficient (i.e. the sudden dip in the Nusselt number vs. the length over the diameter curve) was observed in the studies of [9, 12]. It was of interest to investigate whether the same behavior would occur in the micro-fin tube with the bell-mouth inlet. Therefore, the objective of this study is to analyze the heat transfer characteristics of the micro-fin tube with three different inlet configurations (re-entrant, square-edged, bell-mouth).

NOMENCLATURE

c_p specific heat of the test fluid evaluated at T_b, J/(kg·K)
D_i inside diameter of the test section (tube), m
D_o outside diameter of the test section (tube), m
e internal fin height, mm
h fully developed peripheral heat transfer coefficient, W/(m^2·K)
h_b local peripheral heat transfer coefficient at the bottom of tube, W/(m^2·K)
h_t local peripheral heat transfer coefficient at the top of tube, W/(m^2·K)
j Colburn-j factor [=St $Pr^{0.67}$], dimensionless
k thermal conductivity, evaluated at T_b, W/(m·K)
N_s Number of starts/fins inside the cross-sectional area, dimensionless
Nu local average or fully developed peripheral Nusselt number (= $h \cdot D_i /k$), dimensionless
p axial fin pitch, [=$\pi \cdot D_i /(N_s \cdot \tan \alpha)$], m
Pr local bulk Prandtl number (=$c_p \cdot \mu_b /k$), dimensionless
Re local bulk Reynolds number (=$\rho \cdot V \cdot D_i /\mu_b$), dimensionless
St local average or fully developed peripheral Stanton number [=Nu/(Pr·Re)], dimensionless
T_b local bulk temperature of the test fluid, ºC
V average velocity in the test section, m/s
x local axial distance along the test section from the inlet, m

Greek Symbols

α Spiral angle, degree
μ_b absolute viscosity of the test fluid evaluated at T_b, Pa·s
μ_w absolute viscosity of the test fluid evaluated at T_w, Pa·s
ρ density of the test fluid evaluated at T_b, kg/m^3

Subscripts

l laminar
t turbulent

EXPERIMENTAL SETUP

The heat transfer experimental data used in this study were obtained from the experimental apparatus shown in Figure 1.

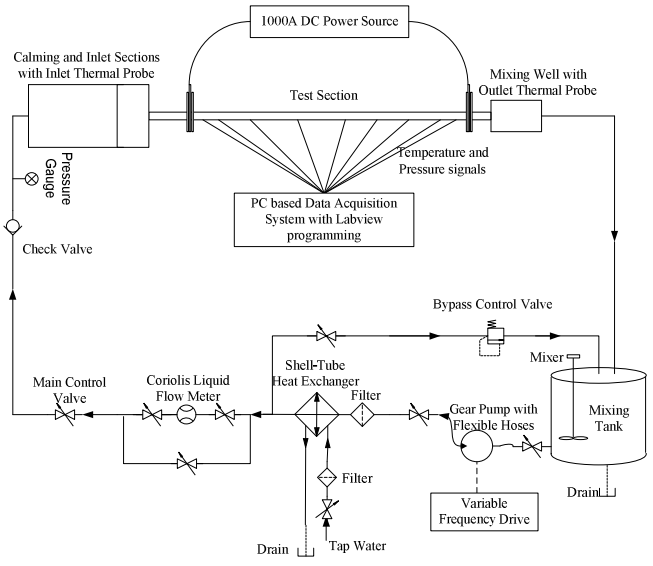

Figure 1: Experimental setup.

The local forced and mixed convective heat transfer measurements were made in a horizontal, electrically heated, copper circular straight tube under uniform wall heat flux boundary condition. As shown in Figure 2, three types of inlet configurations (re-entrant, square-edged and bell-mouth) were installed before the test section. The length of each inlet was 23.5 cm. The re-entrant inlet was simulated by sliding 1.5 cm of the tube entrance length into the inlet section, which was otherwise the square-edged (sudden contraction) inlet. For the bell-mouth inlet, a nozzle had to be constructed to replace the inlet section. The nozzle was designed according to the method suggested by Morel [13] and was constructed of aluminum. The nozzle had an area contraction ratio of 122.6. A calming and inlet section similar to that used in Ghajar and Tam [8] was used to ensure a uniform velocity distribution at the entrance of the test section. Water and a mixture of water and ethylene glycol were used as the test fluid in the closed-loop experimental system. The DC arc welder provided the uniform wall heat flux boundary condition to the test section.

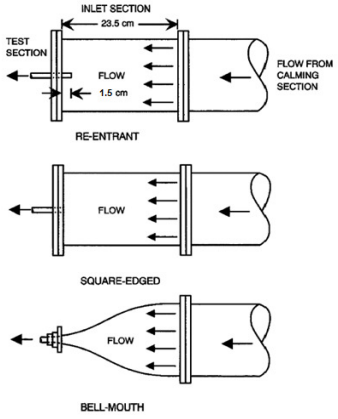

Figure 2: Type of inlet.

In this study, the plain tube and micro-fin tube (see Figure 3) were used as the test section.

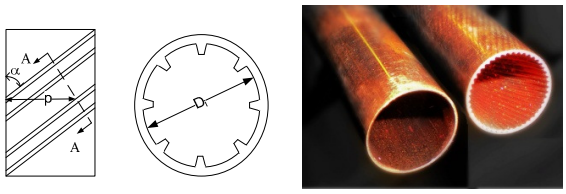

(a) (b)

Figure 3: (a) Sectional view of the micro-fin tube; (b) The plain and micro-fin tubes.

Table 1 represents the specification of the tubes. The tubes have an inside diameter of 14.9 mm and an outside diameter of 15.9 mm. The total length of the test section is 6 m, providing a maximum length-to-inside diameter ratio of 403. The micro-fin tube has an inside surface area enhacement ratio of 1.34 when compared with the plain tube.

Table 1: Specifications of the test tubes.

Tube Type	Outer Dia., D_o (mm)	Inner Dia., D_i (mm)	Spiral angle, α	Fin height, e (mm)	Number of starts, N_s
Plain tube	15.9	14.9	–	–	–
Micro-fin tube	15.9	14.9	35°	0.5	25

As shown in Figure 4, the thermocouples denoted as TC1, TC2, TC3, and TC4, were placed 90° apart around the periphery and the single pressure tap was placed between the TC1 and TC2 thermocouples. The pressure drop data were simulatneously recorded for the friction factor experiments. From the local peripheral wall temperature measurements at each axial location, the inside wall temperatures and the local heat transfer coefficients were calculated by the method shown in Ghajar and Kim [14]. The method used a finite-difference formulation to determine the inside wall temperature and the inside wall heat flux from measurments of the outside wall temperature, the heat generation within the tube wall, and the thermophysical properties of tube materials (electrical resistivity and the thermal conductivity). In these calculations, the axial conduction was assumed negligible (RePr > 4,200 in all cases), but peripheral and radial conduction of heat in the tube wall were included. In addition, the bulk fluid temperature was assumed to increase linearly from the inlet to the outlet. Also, the dimensionless numbers, such as Reynolds, Prandtl, Grashof, and Nusselt numbers were computed by the computer program developed by Ghajar and Kim [14]. In the present study, the experiments covered a local bulk Reynolds number range of 1100 to 23,000, a local Prandtl number range of 4.6 to 46.2, a local bulk Grashof number range of 4376 to 50,519, and a local bulk Nusselt number range of 13.6 to 275.4. The wall heat flux for the experiments ranged from 3.4 to 8.5 kW/m^2.

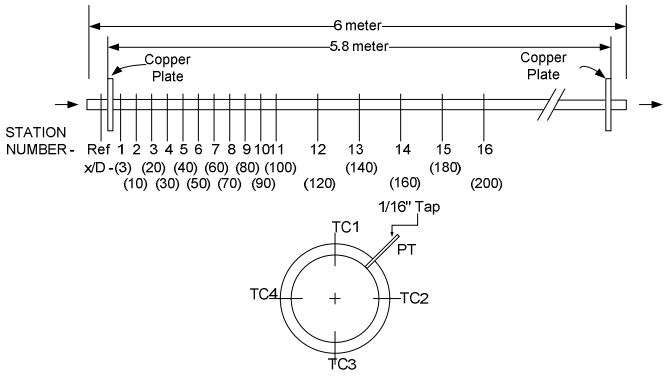

Figure 4: Arrangement of the thermocouples on the test section.

All the thermocouples were calibrated before the experimental runs. The high-precision Coriolis flowmeter was

calibrated by the manufacturer. Table 2 lists the uncertainties of the measured variables and calculated variables over the entire range of Reynolds numbers studied. The calculation method is based on Kline and McClintock [15].

Table 2: Uncertainies in experimental data.

Measured variables		**Calculated variables**	
Variable	**Uncertainty**	**Variable**	**Uncertainty**
Temperature	0.22 °C	*h (heat transfer coefficient)*	20.5%
Mass flow rate	0.77% of full range (0.3-30USGPM)	*Nu (Nusselt number)*	20.5%
Density	0.2 kg/m^3		
Diameter	0.02mm		
Length	0.1mm		
Voltage	1%		
Current	1%		

RESULTS AND DISCUSSION

To verify the new experimental setup and later to compare with the micro-fin tube data, experiments for plain tube were conducted first. Figure 5 shows the recently collected plain tube heat transfer data for the three different inlets compared with those collected by Ghajar and Tam [8]. Since the deviations between the new data and old data were below ±15%, the experimental setup and the data were confirmed to be reliable. It should be noted that the parallel shift from the classical fully developed value of Nu = 4.364 for uniform wall heat flux boundary condition in the laminar region is due to the buoyancy effect and it will be explained later.

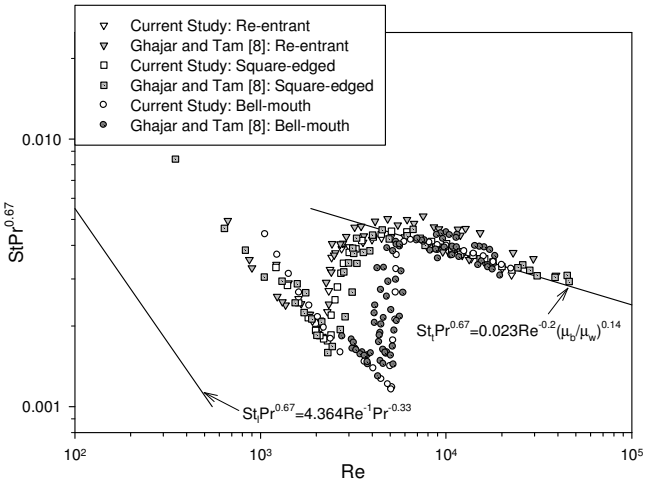

Figure 5: Heat transfer characteristics for the plain tube at x/D_i of 200.

After the verifications of the experimental setup, heat transfer data for the micro-fin tube were measured in a single test section. The plain and micro-fin tubes results are shown in Figure 6. As seen in this figure, the start and end of transition for heat transfer (with uniform wall heat flux boundary condition) in plain and micro-fin tube for the three inlet configurations (re-entrant, square-edged and bell-mouth) were established. The transition Reynolds numbers for heat transfer are summarized in Table 3. The start and end of the transition region can be clearly observed from Figure 6. The start of transition for both plain and micro-fin tubes is defined as the point of sudden departure from the laminar Nu line parallel to the classical Nu = 4.364 line. And, the end of the transition for the plain tube is the first point where the heat transfer data landed on the Sieder and Tate's [16] correlation line and for the micro-fin tube is defined as the first point where the heat transfer data landed on a line parallel to the Sieder and Tate's correlation.

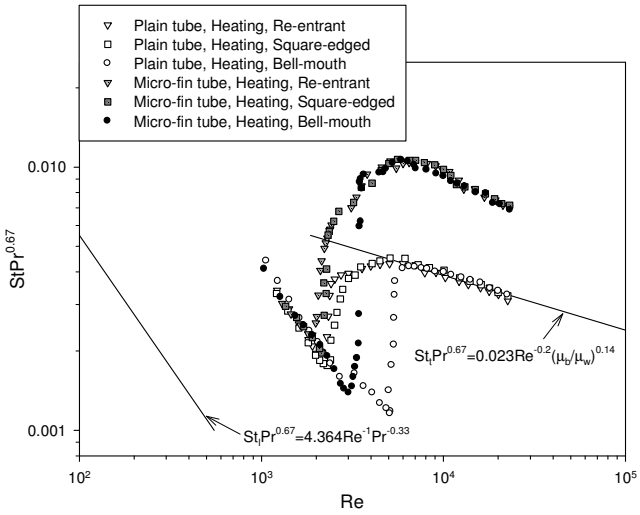

Figure 6: Heat transfer characteristics for the plain and micro-fin tubes at x/D_i of 200.

In Figure 6, it can be seen that the heat transfer data of the plain and micro-fin tubes in the laminar region are comparable and collapse into a single line parallel to the classical laminar fully developed line (Nu = 4.364 for uniform wall heat flux boundary condition). The shift from the classical value is caused by the buoyancy effect. The buoyancy effect for the micro-fin tube can also be examined by the ratio of the heat transfer coefficient of the top and bottom (h_t/h_b) as was demonstrated by Ghajar and Tam [8, 17] for plain tube. As seen in Figure 4, four thermocouples are used at each location. According to the plain tube studies [8, 17], the ratio of h_t/h_b should be close to unity (0.8–1.0) for forced convection and is much less than unity (<0.8) for a case in which mixed convection exists. As seen in Figure 7, for the micro-fin tube with re-entrant and square-edged inlets when the Reynolds number is less than 2000 and 2200, respectively, the ratio of h_t/h_b starts at one and decreases rapidly and finally stabilizes when x/D_i is larger than 100. According to Table 3, the lower

transition Reynolds number for the micro-fin tubes with these two inlets is almost the same as the plain tube (1964 vs. 2001 for re-entrant, 2144 vs. 2298 for square-edged). The direct effect of the presence of buoyancy forces in the laminar region is the main reason for the parallel shift from the classical Nu value of 4.364 observed in Figures 5 and 6. No buoyancy effect is observed in the transition and turbulent regions. For the micro-fin tube with a bell-mouth inlet, the buoyancy effect occurs when the Reynolds number is less than 3000, the ratio of h_t/h_b starts at one and decreases rapidly and finally stabilizes when x/D_i is larger than 100. As shown in Table 3, the lower transition Reynolds number for this inlet is advanced to 3015 for the micro-fin tube from 5082 for the plain tube. Therefore, for the bell-mouth inlet, the buoyancy effect is also observed in the laminar region only.

Table 3: Start and end of transition for the plain and micro-fin tubes at x/D_i of 200.

Tube, Inlet	Heat Transfer			
	Re_{start}	$StPr^{0.7}$	Re_{end}	$StPr^{0.7}$
Plain, Re-entrant	2001	2.0e-3	7919	4.1e-3
Plain, Square-edged	2298	1.8e-3	8357	4.1e-3
Plain, Bell-mouth	5082	1.2e-3	8162	4.1e-3
Micro-fin, Re-entrant	1946	2.3e-3	8105	10.3e-3
Micro-fin, Square-edged	2144	2.0e-3	8254	10.3e-3
Micro-fin, Bell-mouth	3015	1.4e-3	8092	9.8e-3

As shown in Figure 6, for the micro-fin tube, it can be observed that the start of transition is found to be inlet dependent. The start of transition Reynolds number for each inlet is determined to be about 2000 for the re-entrant, 2100 for square-edged, and 3000 for the bell-mouth inlets. The results indicate that the re-entrant inlet configuration causes the earliest transition, while the bell-mouth inlet delays the start of transition. The square-edged inlet falls in between. Referring to Table 3 and Figure 6, for the plain tube, the lower transition Reynolds number for the re-entrant, square-edged, and bell-mouth inlets is 2001, 2298 and 5082, respectively. For micro-fin tube, the lower transition Reynolds number reduced to 1946 for the square-edged inlet, 2144 for the re-entrant inlet, and 3015 for the bell-mouth inlet. Therefore, it can be observed for both square-edged and re-entrant inlets that the lower transition Reynolds number of the micro-fin tube is almost the same as that of the plain tube. However, the lower transition Reynolds number for the bell-mouth inlet is obviously advanced by the micro-fins. For the upper transition Reynolds number for the micro-fin tube, they were 8105 for the re-entrant, 8254 for the square-edged and 8092 for the bell-mouth, and therefore, the upper transition is almost the same for all three types of inlet configurations when compared with the plain tube (Re = 7919 for re-entrant, Re = 8357 for square-edged, and Re = 8162 for bell-mouth).

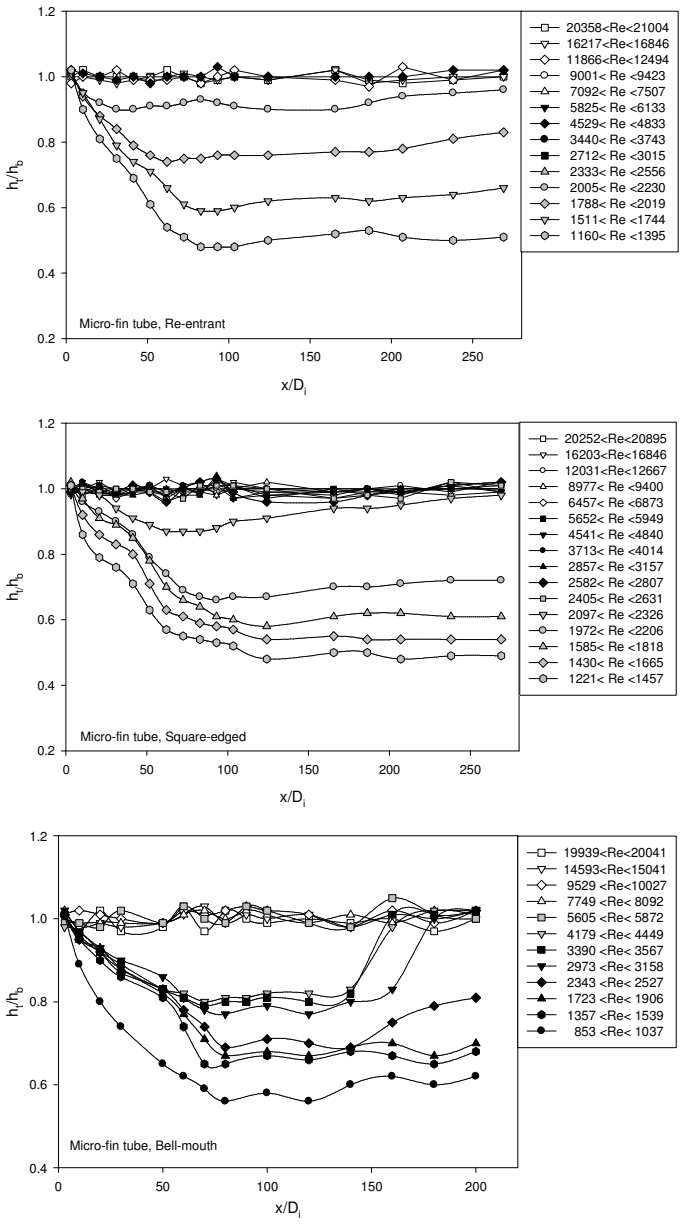

Figure 7: The ratio of heat transfer coefficients at the top and bottom on the micro-fin tube with different inlets.

Referring to Figure 6, it was observed, for the micro-fin tube, the heat transfer enhancement initiated in the transition region and lasted through the turbulent region. Around Reynolds number of 8000 the plain tube data follows the Sieder and Tate correlation [16] for the turbulent region. However, the micro-fin data continued to increase up to a Reynolds number of about 8000 and then made a parallel shift from the Sieder and Tate correlation. This increase in the Colburn j factor ($St\ Pr^{0.67}$) and the parallel shift from the Sieder and Tate correlation in the turbulent region is due to the the increase in inside

surface area and the swirling motion induced by the spiral micro-fins. According to Webb et al. [18], the mechanism of the heat transfer enhancemnent is that the micro-fin increases both the surface area and the fluid mixing between the bulk fluid and the tube wall.

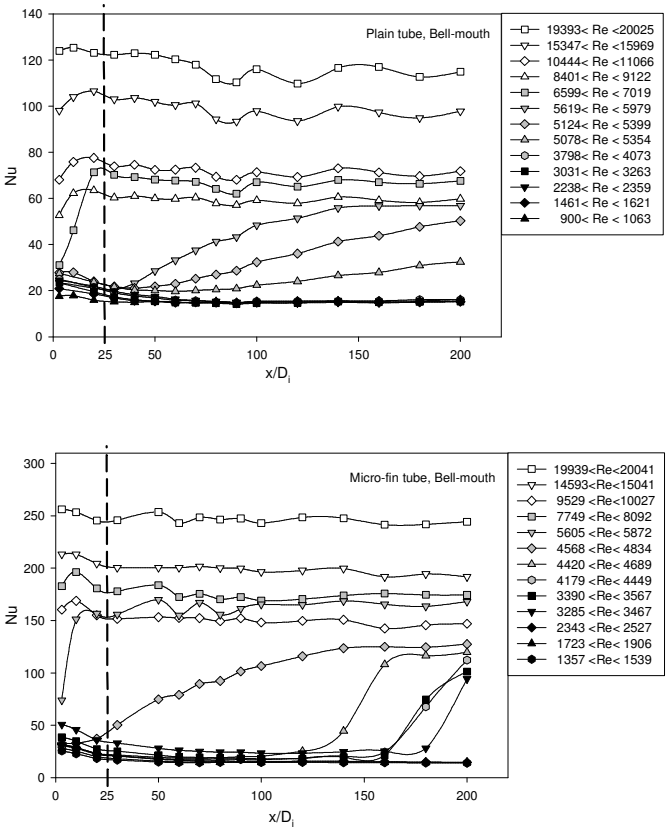

Figure 8: Variation of local Nusselt number with length for the plain tube and micro-fin tube with the bell-mouth inlet.

Figure 8 shows the variation of local Nusselt number along the tube length (x/D_i) in the entire flow regime (laminar, transition, turbulent) for the plain and micro-fin tubes with the bell-mouth inlet configuration. As shown in Figure 8, for both the plain and micro-fin tubes, the variation of the local heat transfer coefficient with tube length in the transition and turbulent regions is unusual. For the laminar region, the local Nussult number first decreases along the tube and then stays constant after x/D_i of 100. However, for the transition region, the local Nussult number first decreases along the tube, reaches the minimum value and then increases. Therefore, the dip in the Nu vs. x/D_i curve can be observed. In fact, the dip also occurs in the turbulent region. In case the dip cannot be observed in the turbulent region, it simply implies that this characteristic disappears very near the entrance of the tube ($x/D_i < 25$). Therefore, the length of dip in the turbulent region ($x/D_i < 25$) is much shorter than that in the transition region ($40 < x/D_i < 150$). The unusual behavior observed in the current study is matched with the findings of [9, 12]. As explained by [9, 12], for the plain tube with a bell-mouth inlet, the boundary layer along the tube wall is at first laminar and then changes through a transition to the turbulent condition, causing a dip in the Nu vs. x/D_i curve. Furthermore, the length of dip in the turbulent region is also shorter than that of the transition region.

CONCLUSIONS

In this study, heat transfer for horizontal plain and micro-fin tubes with three different inlet configurations were obtained under uniform wall heat flux boundary condition. From the results, the following conclusions can be made:

- For the plain and micro-fin tubes with three types of inlets, the buoyancy effect was present in the laminar region.
- For the plain and micro-fin tubes, the start of transition was inlet dependent. The re-entrant inlet had the earliest start of transition and the bell-mouth inlet had the latest one. The square-edged inlet fell in between.
- For the bell-mouth inlet, the start of transition was advanced by the micro-fins.
- Regardless of the type of inlet, a parallel shift in the heat transfer characteristic for the micro-fin tube due to the surface area increase and swirling motion induced by the micro-fins was observed in the turbulent region.
- For both of the plain and micro-fin tubes with bell-mouth inlet, the unusual behavior in the Nu vs. x/D_i curve was observed in the transition and turbulent regions.

ACKNOWLEDGMENTS

This research is supported by the Institute for the Development and Quality, Macau.

REFERENCES

[1] Jensen, M. K., and Vlakancic, A., 1999, "Technical note – Experimental investigation of turbulent heat transfer and fluid flow in internally finned tubes," International Journal of Heat and Mass Transfer, 42(7), pp. 1343-1351.

[2] Khanpara, J. C., Bergles, A. E., and Pate, M. B., 1986, "Augmentation of R-113 in tube evaporation with microfin tubes," ASHRAE Transactions, 92(2b), pp. 506-524.

[3] Brognaux, L. B., Webb, R. L., and Chamra, L. M., 1997, "Single phase heat transfer in micro-fin tubes," International Journal of Heat and Mass Transfer, 40(18), pp. 4345-4357.

[4] Esen, E. B., Obot, N. T., and Rabas, T. J., 1994, "Enhancement: Part I. Heat transfer and pressure drop results for air flow through passages with spirally-shaped roughness," Journal of Enhanced Heat Transfer, 1(2), pp. 145-156.

[5] Shome, B., and Jensen, M. K., 1996, "Experimental investigation of laminar flow and heat transfer in internally finned tubes," Journal of Enhanced Heat Transfer, 4(1), pp. 53-70.

[6] Al-Fahed, S., Chamra, L. M., and Chakroun, W., 1999, "Pressure drop and heat transfer comparison for both microfin

tube and twisted tape inserts in laminar flow," Experimental Thermal and Fluid Science, 18(4), pp. 232-333.
[7] Trupp, A. C., and Haine, H., 1989, "Experimental investigation of turbulent mixed convection in horizontal tubes with longitudinal internal fins," National Heat Transfer Conference, Philadelphia, PA, HTD-Vol. 107, Heat Transfer in Convective Flows.
[8] Ghajar, A. J., and Tam, L. M., 1994, "Heat transfer measurements and correlations in the transition region for a circular tube with three different inlet configurations," Experimental Thermal and Fluid Science, 8(1), pp. 79-90.
[9] Tam, L. M., and Ghajar, A. J., 1998, "The unusual behavior of local heat transfer coefficient in a circular tube with a bell-mouth inlet," Experimental Thermal and Fluid Science, 16(3), pp. 187-194.
[10] Tam, L. M., and Ghajar, A. J., 2006, "Transitional Heat Transfer in Plain Horizontal Tubes," Heat Transfer Engineering, 27(5), pp 23-38.
[11] Tam, H. K., Tam, L. M., and Ghajar, A. J., 2011, "Experimental Analysis of the Single-Phase Heat Transfer and Friction Factor inside the Horizontally Micro-Fin Tube," Proceedings of ASME/JSME 2011(AJTE2011) 8th Thermal Engineering Joint Conference, Honolulu, Hawaii, March 14-17, 2011.
[12] Al-Arabi, M., 1982, "Turbulent heat transfer in the entrance region of a tube," Heat Transfer Engineering, 3(3-4), pp. 76-83.
[13] Morel, T., 1975, "Comprehensive Design of Axisymmetric Wind Tunnel Contractions," Trans. ASME J. Fluids Eng., 97(2), pp. 225-233.
[14] Ghajar, A. J., and Kim, J., 2006, "Calculation of local inside-wall convective heat transfer parameters from measurements of the local outside-wall temperatures along an electrically heated circular tube," Heat Transfer Calculations, edited by Myer Kutz, McGraw-Hill, New York, NY, pp. 23.3-23.27.
[15] Kline, S. J., and McClintock, F. A., 1953, "Describing Uncertainties in Single Sample Experiments," Mech. Eng., 75(1), pp. 3-8.
[16] Sieder, E. N., and Tate, G. E., 1936, "Heat Transfer and Pressure Drop in Liquids in Tubes," Ind. Eng. Chem., 28, pp. 1429-1435.
[17] Ghajar, A. J., and Tam, L. M., 1995, "Flow regime map for a horizontal pipe with uniform wall heat flux and three inlet configurations," Experimental Thermal and Fluid Science, 10, pp. 287–297.
[18] Webb, R. L., Narayanamurthy, R., and Thors, P., 2000, "Heat transfer and friction characteristics of internal helical-rib roughness", Journal of Heat Transfer, 122(1), pp. 134-142.